Design of a passive dispersive filter for analog pulse compression radar

Hanane Meliani, Emilie Avignon-Meseldzija, Jelena Anastasov, Dejana Milić, Pietro M. Ferreira

Design of a Passive Dispersive Filter for Analog Pulse Compression Radar

Hanane Meliani, Emilie Avignon-Meseldzija, Jelena Anastasov, Dejan Milic, Pietro Maris Ferreira

***Abstract*—The paper presents the design of a dispersive filter for an analog pulse compression radar. The architecture of the analog pulse compression radar is presented with its equations, limitations, trade-off and architecture comparison with the more traditional FMCW radar. In the past decades, the matched filter of analog pulse compression radar has been implemented with SAW filters, having a reduced bandwidth and then poor resolution. Here the matched filter is designed with a passive dispersive filter instead of a SAW. The design of the filter is described, measured, and compared to the state-of-the-art of dispersive filter. The use of wideband passive analog matched filter paves the way to better signal-to-noise ratio and reduced power consumption compared to its traditional FMCW counterpart. The measured filter, composed of 2 passive cells achieved with components of the shelves has a group delay downslope of -1 ns/GHz which is one of the strongest downslope reported in the literature. The considered bandwidth is [700MHz – 1.9GHz].**

***Keywords*—dispersive filter, analog pulse compression, matched filter, radar**

I. Introduction

In the context of IoT, high-resolution radar detection in embedded system is a critical issue in numerous applications like: snow thickness measurement for climate change monitoring in Arctic environment [1]–[3], remote vital signs monitoring [4], [5] and embedded short-range detection in general [6]. For embedded short-range detection, FMCW (Frequency Modulated Continuous Wave) radars are generally preferred to their pulse-radar counterpart due to the relative simplicity to emit a chirp signal compared to a short-time high-power pulse. In a large majority of FMCW radar architectures, the sent chirp is multiplied with the received chirp to obtain a beat signal whose the frequency is proportional to the distance [1]–[6]. The beat signal is then digitized and processed in the frequency domain, most of the time by FFT. An alternative to the architecture with the multiplier is the one with an analog matched filter. The SAW (Surface Acoustic Wave) filters are a way to create this matched filter but are also limited to few megahertz bandwidth [7]. In this context, it is interesting to consider latest development in Analog Signal Processing (ASP). For example, in the work presented in [8], communication pulses are transformed through a phaser (i.e dispersive filter) into UWB (Ultra Wide Band) signals whose properties depends on the phasers properties. Thus, only an appropriate phaser, mathematically calculated, can retrieve the original signal. It is a temporal expansion paving the way to UWB fully-analog communication. In optical communication, where there is a need for sharp optical pulses, the tendency is to time compression. To obtain such pulses a technique consists in using a wideband optical chirp and to compress it with various optical devices [9], [10]. In these reference it is explained that the larger the bandwidth of the chirp the sharper the pulse.

In what comes next, we propose to design a downslope dispersive filter to later implement the concept of time compression used in [8] and [9] to create a matched filter for a chirp radar. To implement such a filter two cells are optimized with the method published in [11] and we use components of the shelves soldered on PCBs.

The paper is organized as follows: Section II presents the architecture of the targeted analog pulse compression radar with equations and limitation. Section III presents an optimized downslope dispersive filter suitable for this kind of application and Section IV presents measurement results of the realized filter.

II. Analog Pulse Compression Radar

A. Principle of the analog pulse compression radar

The analog pulse compression radar is presented in Fig. 1. The emitter of the analog pulse compression radar is composed of a chirp generator creating the signal $s(t)$ and a PA (Power Amplifier). The receiver is composed of a LNA (Low Noise Amplifier) and an analog matched filter. Ideally the analog matched filter is a filter whose impulse response $h(t)$ is a complex-conjugated and time-reversed version of $s(t)$. The group delay $\tau(f)$ of the matched filter must attributes a specific delay to each frequency in order to achieve the compression. For example, if we have a linear up-chirp signal $s(t)$, then the group delay $\tau(f)$ of the matched filter must be with linear negative slope. At the output of the matched filter we obtain a pulse corresponding to the time reference due to the chirp applied without delay and pulses corresponding to delayed chirps from target feedbacks. To exploit this output, it is

First, second and last Authors are with Université Paris-Saclay, CentraleSupélec, Sorbonne-Université, CNRS, Lab. de Génie Electrique et Electronique de Paris (e-mail: first.author@centralesupelec.fr).

Second and Third Author are with the School of Electrical Engineering, University of Belgrade, Bulevar kralja Aleksandra 73, 11000 Belgrade, Serbia (e-mails: second.author@elfak.ni.ac.rs, third.author@elfak.ni.ac.rs).

979-8-3503-4702-9/23/$31.00 ©2023 IEEE

possible to place a comparator and a counter to evaluate the delay *2d/c* proportional to the distance *d*.

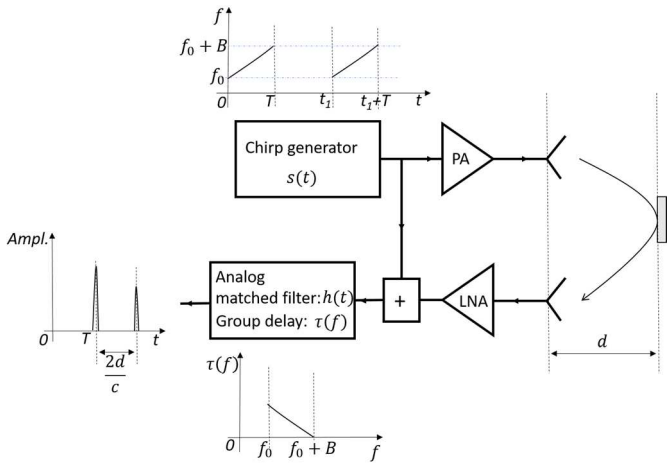

Fig. 1 Proposed Analog Pulse Compression Radar

B. *Equations and limitations*

For the sake of simplicity, we will consider all the signals as ideal complex signals (manipulating exponential signal is easier and is the ideal reference). The transmitted up-chirp signal is:

$$s(t) = Ae^{i2\pi\left(f_0 t+\frac{1}{2}at^2\right)} \quad (1)$$

where f_0 is the initial frequency of the chirp and a is the ratio B/T with B the bandwidth of the chirp and T the sweep time of the chirp. Let's consider that the chirp is reflected by a target at a distance d, corresponding to a delay in the received chirp $\tau_0 = 2d/c$. Then, we have at the input of the matched filter:

$$e(t) = Ae^{i2\pi\left(f_0 t+\frac{1}{2}at^2\right)} + A_0 e^{i2\pi\left(f_0(t-\tau_0)+\frac{1}{2}a(t-\tau_0)^2\right)} \quad (2)$$

The impulse response of the matched filter is:

$$h(t) = e^{i2\pi\left(f_2 t-\frac{1}{2}at^2\right)} \quad (3)$$

where $f_2 = f_0 + B$. The output of the filter *Out(t)* is then the convolution of *h(t)* with *e(t)*:

$$Out(t) = \int_0^{2T} h(x)e(t-x)dx \quad (4)$$

Leading to: $s(t) = Ae^{i2\pi\left(f_0 t+\frac{1}{2}at^2\right)}sinc\big(2B(T-t)\big) + A_0 e^{i2\pi\left(f_0(t-\tau_0)+\frac{1}{2}a(t-\tau_0)^2\right)}sinc\big(2B(T-t+\tau_0)\big)$ (5)

From (5), it can be observed that the output signal of the matched filter is composed of two *Sinc* functions. One *Sinc* is centered around *T* and is the time reference for the radar, and the other *Sinc* is centered around T + τ_0. So the time difference between the maximum of the two *Sinc* is the delay to the target. The distance to the target is then deduced by: $d = \tau_0 c/2$. Due to the distance to the target, the amplitude of the signal reflected by the target is attenuated, this is why the second pulse is always smaller than the reference.

Figure 2 presents the output of the analog matched for two different chirp bandwidth *B*: 1.5 GHz and 5 GHz. The other parameters are: T = 10ns, f_0 = 100 MHz, A = 1, A0 = 0.7 and a distance to the target d = 30 cm corresponding to a τ_0 of 2 ns. As it is predictable from (5) based on *Sinc* function, the principal lobe width decreases with increased chirp bandwidth B. It means that the largest the bandwidth of chirp and matched filter, the better the resolution (i.e as in FMCW radar). One of the limitation in analog pulse compression radar is the achievable bandwidth of the matched filter.

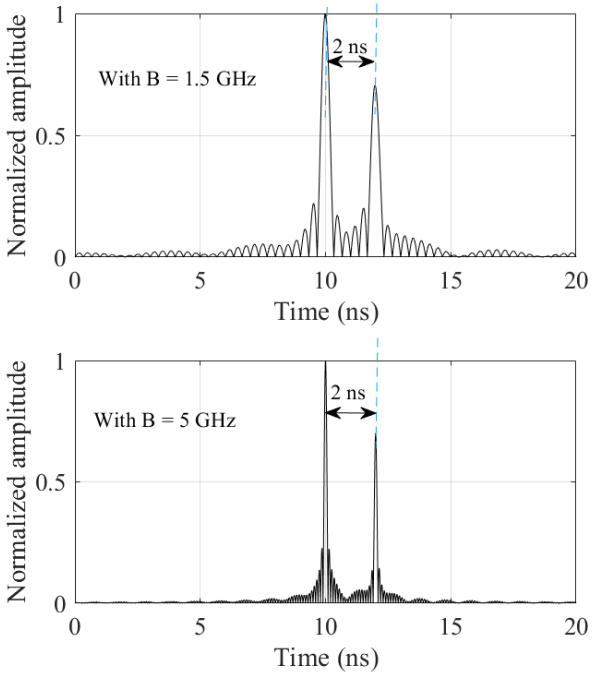

Fig. 2: Output of analog matched filter sith B = 1.5 GHz (up) and B = 5 GHz (down)

In what follows we describe the design of a possible matched filter with a bandwidth of 1.3 GHz which is achievable with discrete components and a PCB.

III. DESCRIPTION OF THE ANALOG MATCHED FILTER

A. *Optimization of the matched filter*

The matched filter is a dispersive filter, more particularly with a linear group delay. To calculate the cascade of suitable all-pass cells we will use the most recent and robust mathematical method presented in [11]. This method has been used already to optimize the positive slope active dispersive filters presented in [12]. For a two cells cascade of downslope dispersive filter on the bandwidth [700 MHz – 2 GHz], optimal parameters are proposed in Table I. In this table the f_{0i} and Q_i refer to the center frequency and quality factor of general second order all pass cell having the transfer function given by (6). The group delay of this filter is the derivative of the phase response with respect to ω, and can be expressed as (7) in accordance with [13, (7-11)]. This kind of filter can be obtained with a passive approach like presented in [11] or with an active approach like in [12]. In this work we selected the passive approach and the synthesis is described in the next paragraph.

TABLE I
OPTIMIZED PARAMETERS

Cell *i*	f_{0i} (MHz)	Q_i
1	800.698	1.1099
2	1368.9	1.2242

As soon as the filter have the same input and output impedance, the cascade of the filter will result for the group delay as the sum of the group delay of each cell. The individual group delay of each cell as well as the expected group delay of the cascade are presented in Fig. 3. From this figure, we can observe that the group delay is linear from 780 MHz up to 1.9 GHz with a downslope of -1 ns/GHz.

$$H_i(j\omega) = \frac{-\omega^2 - j\omega\frac{\omega_{0i}}{Q_i} + \omega_{0i}^2}{-\omega^2 + j\omega\frac{\omega_{0i}}{Q_i} + \omega_{0i}^2} \quad (6)$$

$$\tau_i(\omega) = 2\omega_{0i}Q_i \frac{\omega^2 + \omega_{0i}^2}{\omega^2\omega_{0i}^2 + Q_i^2(\omega^2 - \omega_{0i}^2)^2}. \quad (7)$$

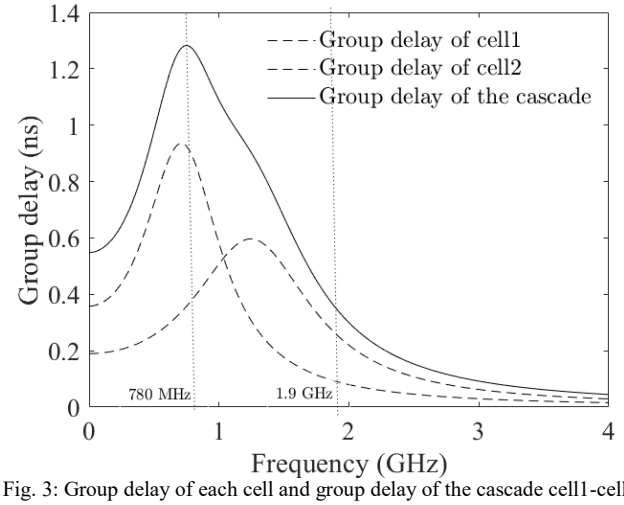

Fig. 3: Group delay of each cell and group delay of the cascade cell1-cell2

B. *Components calculation*

The passive topology used for the design of each second-order low-pass cell is presented in Fig. 4. To obtain the wanted group delay based on the values of f_{0i} and Q_i, we use the formulas provided in [14], which are:

$$L_1 = \frac{RQ_i}{\omega_{0i}} \quad (8)$$

$$L_2 = \frac{R}{Q_i\omega_{0i}} \quad (9)$$

$$C_1 = \frac{1}{RQ_i\omega_{0i}} \quad (10)$$

$$C_2 = \frac{Q_i}{\omega_{0i}R} \quad (11)$$

where R is the wanted value of input and output impedance, here 50 Ω. Resulting calculated nominal values are synthesized in Table II together with the selected SMD components which have been selected. These selected components are the one with the closest value available in the market. The view of one cell is presented in Fig. 5.

TABLE II
IDEAL VALUES VS SMD COMPONENTS VALUES

	Cell i	$2L_2$ (nH)	$L_1/2$ (nH)	C_1 (pF)	$(C_2-C_1)/2$ (pF)
Ideal	1	17.6	5.5	3.6	0.4
	2	10.5	3.2	2	0.24
SMD	1	18	4.7	3.3	0.5
	2	10	2.7	2.2	0.3

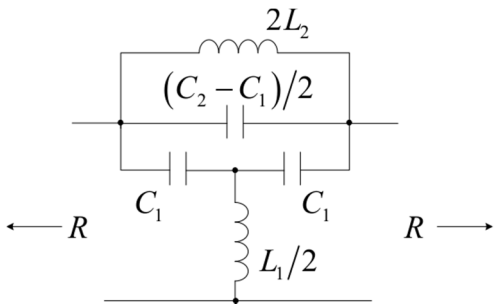

Fig. 4: Selected passive bridge-T topology for the second-order all-pass filter

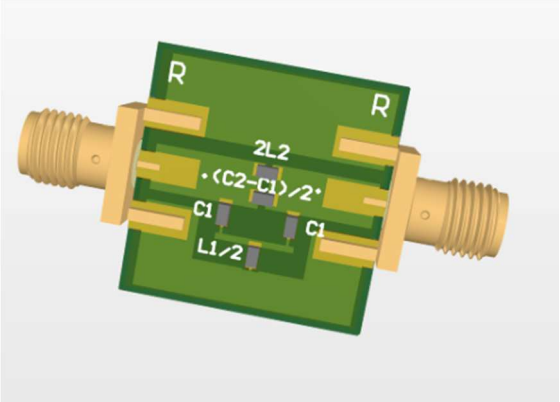

Fig. 5: View of one bridge-T cell with sma connectors

IV. MEASUREMENT OF THE DISPERSIVE FILTER

A picture of the prototype is presented in Fig. 6. The cells are cascaded with SMA male connectors and the circuit has been measured with a Rhode and Schwarz ZND vector network analyzer. Calibration has been done with N connectors and TOSM (Through-Open-Short-Match) Cal-Kit. For measurement, two N/SMA adapters have been added after calibration and are connected to the VNA through 60 cm Radiall cables. Group delay is measured using aperture width of 5%. The resulting group delay is presented in Fig. 7, while S-parameters are presented in Fig. 8. It can be observed from Fig. 7 that the shape of the measured group delay totally fits with the ideal expected group delay. A residual group delay offset exists and is due to the two N/SMA adapters and the length of the lines in the prototype. The bandwidth of linear-shape of the group delay is as predicted from 780 MHz up to 1.9 GHz and goes on to 2.3 GHz. As predicted the downslope of the group delay is -1 ns/GHz. S-parameters show a suitable matching up to 1.8 GHz with S_{11} and S_{22} parameters remaining below -10 dB.

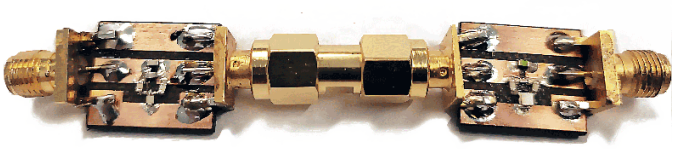

Fig. 6: Two-cells prototype

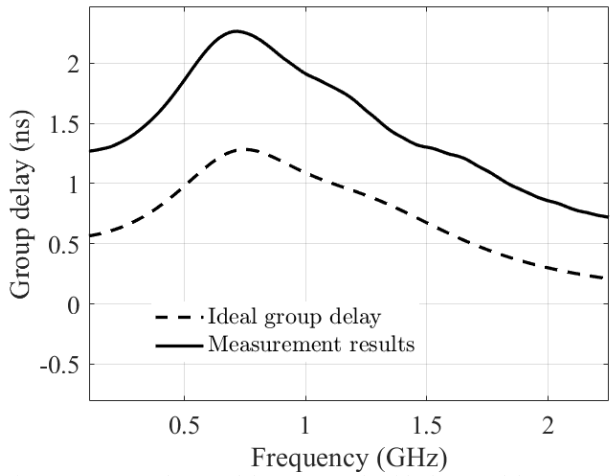

Figure 7: Measured group delay compared to ideal group delay

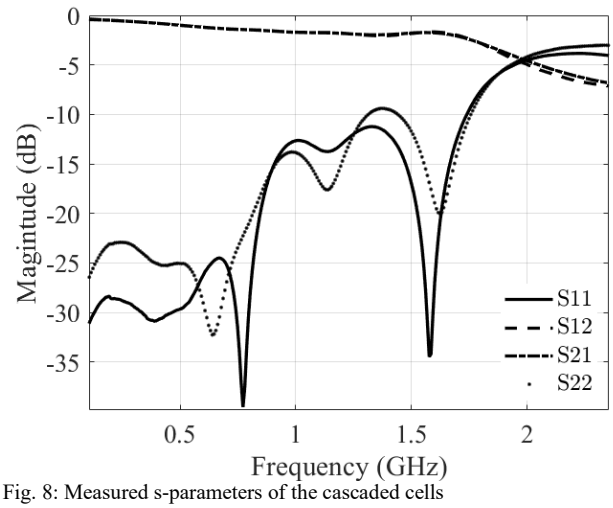

Fig. 8: Measured s-parameters of the cascaded cells

V. Conclusion

In this paper a dispersive filter with a downslope linear group delay characteristic has been designed based on a cascade of two optimized second order passive all-pass cells. Measurement results show a useful bandwidth from 780 MHz up to 1.9 GHz, with a downslope -1 ns/GHz. The targeted application for this kind of filter is analog pulse compression radar which is described with equations and limitations in the first part of the paper. While there is still space for improving linearity, measurement results indicate that this kind of dispersive filters can be successfully implemented using lumped elements in lower gigahertz range of frequencies.

References

[1] A. Jutila, J. King, J. Paden, R. Ricker, S. Hendricks, C. Polashenski,V. Helm, T. Binder, and C. Haas, “High-resolution snow depth on arctic sea ice from low-altitude airborne microwave radar data,” IEEE Transactions on Geoscience and Remote Sensing, vol. 60, pp. 1–16, 2022.

[2] Y. Kim, T. J. Reck, M. Alonso-delPino, T. H. Painter, H.-P. Marshall, E. H. Bair, J. Dozier, G. Chattopadhyay, K.-N. Liou, M.-C. F. Chang, and A. Tang, “A ku-band cmos fmcw radar transceiver for snowpack remote sensing,” IEEE Transactions on Microwave Theory and Techniques, vol. 66, no. 5, pp. 2480–2494, 2018.

[3] J.-B. Yan, D. Gomez-Garcıa Alvestegui, J. W. McDaniel, Y. Li, S. Gogineni,F. Rodriguez-Morales, J. Brozena, and C. J. Leuschen, “Ultrawideband FMCW radar for airborne measurements of snow over sea ice and land,” IEEE Transactions on Geoscience and Remote Sensing, vol. 55, no. 2, pp. 834–843, 2017.

[4] L. Sun, S. Huang, Y. Li, C. Gu, H. Pan, H. Hong, and X. Zhu, “Remote measurement of human vital signs based on joint-range adaptive EEMD,” IEEE Access, vol. 8, pp. 68 514–68 524, 2020.

[5] W. Lv, Y. Zhao, W. Zhang, W. Liu, A. Hu, and J. Miao, “Remote measurement of short-term heart rate with narrow beam millimeter wave radar,” IEEE Access, vol. 9, pp. 165 049–165 058, 2021.

[6] I. M. Milosavljevic, D. P. Glavonjic, D. P. Kr˘cum, S. P. Jovanovic, V. R. Mihajlovic, and V. M. Milovanovi´c, “A 55–64-GHz fully integrated miniaturized FMCW radar sensor module for short-range applications,” IEEE Microwave and Wireless Components Letters, vol. 29, no. 10, pp. 677–679, 2019.

[7] P. Tortoli, F. Guidi, and C. Atzeni, “Digital vs. SAW matched filter implementation for radar pulse compression,” in 1994 Proceedings of IEEE Ultrasonics Symposium, vol. 1, 1994, pp. 199–202 vol.1.

[8] L. Zou, S. Gupta, and C. Caloz, “Real-time dispersion code multiple access for high-speed wireless communications,” IEEE Transactions on Wireless Communications, vol. 17, no. 1, pp. 266–281, 2018.

[9] K. Kashiwagi, Y. Kodama, Y. Tanaka, and T. Kurokawa, “Tunable pulse compression technique using optical pulse synthesizer,” in 2009 Conference on Lasers and Electro-Optics and 2009 Conference on Quantum electronics and Laser Science Conference, 2009, pp. 1–2.

[10] C. Song, J. Qian, M. Lei, Z. Zheng, S. Huang, and X. Gao, “A chirprate-tunable microwave photonic pulse compression system for multioctave linearly chirped microwave waveform,” IEEE Photonics Journal, vol. 11, no. 2, pp. 1–13, 2019.

[11] D. N. Milic, E. Avignon-Meseldzija, J. A. Anastasov, H. Meliani, and A. Benlarbi-Delaï, “A robust algorithm for the design of wideband positive-slope linear group delay filters,” IEEE Transactions on Circuits and Systems I: Regular Papers, vol. 69, no. 10, pp. 4258–4271, 2022.

[12] E. Avignon-Meseldzija, J. Anastasov, and D. N. Milic, “A linear group delay filter with tunable positive slope for analog signal processing,” International Journal of Circuit Theory and Applications, vol. 49, no. 5, pp. 1307–1326, 2021.

[13] A. Williams and F. J. Taylor, Electronic Filter Design Handbook, Fourth Edition (McGraw-Hill Handbooks). McGraw-Hill Professional, 2006.

[14] G. Lissorgues and C. Berland, “Synthèse des filtres LC,” Techniques de l’ingénieur, no. E130, Sep. 2015.